

Expansion of iridaborane clusters by addition of monoborane. Novel metallaboranes and mechanistic detail†‡

Sundargopal Ghosh,^{*a} Bruce C. Noll^b and Thomas P. Fehlner^{*b}

Received 8th October 2007, Accepted 21st November 2007

First published as an Advance Article on the web 12th December 2007

DOI: 10.1039/b715040g

This work reports the results of a thermally driven cluster expansion of *arachno*-1- $\{\eta^5\text{-C}_5\text{Me}_5\text{IrH}_2\}\text{B}_3\text{H}_7$, **1**, with $\text{BH}_3\cdot\text{THF}$. In addition to the previously reported product, *arachno*-1- $\{\eta^5\text{-C}_5\text{Me}_5\text{IrH}\}\text{B}_4\text{H}_9$, **2**, formed at lower temperatures, reaction at 100 °C permits the isolation of four new iridaboranes. Two products, *nido*-1- $(\eta^5\text{-C}_5\text{Me}_5\text{Ir})\text{B}_5\text{H}_9$, **3**, and *nido*-3- $(\eta^5\text{-C}_5\text{Me}_5\text{Ir})\text{B}_9\text{H}_{13}$, **4**, contain a single Ir atom and five and nine framework boron atoms, respectively. One, *nido*-3,4- $(\eta^5\text{-C}_5\text{Me}_5\text{Ir})_2\text{B}_8\text{H}_{12}$, **5**, contains two Ir atoms and eight framework boron atoms. Their structures are predicted by the electron counting rules to be a *nido*-iridahexaborane, **3**, *nido*-iridadecaborane, **4**, and *nido*-diiridadecaborane, **5**. The accuracy of these predictions in each case is established experimentally by spectroscopic characterization in solution and structure determinations in the solid state. A less stable metallaborane has been identified and the available spectroscopic and crystallographic information are consistent with the formulation *nido*-3,4- $(\eta^5\text{-C}_5\text{Me}_5\text{Ir})_2\text{B}_8\text{H}_{13}(\mu\text{-BH}_2)$, **6**, *i.e.*, a species containing an exopolyhedral bridging BH group. These new observations, along with earlier ones on ruthenaborane cluster systems, are used to fully define a general mechanism for a cluster expansion reaction, *i.e.*, addition of borane to form an exopolyhedral adduct followed by cage insertion.

Introduction

Metallaborane chemistry is an interesting and diverse area of cluster chemistry which is closely allied to both polyhedral metal compounds as well as boron hydrides.^{1–17} Developments in this chemistry continue to demonstrate that close electronic and structural relationships exist between organometallic compounds and those formed from metal and polyhedral borane fragments despite the fact that “electron deficient” boranes are not considered ligands in the normal sense of coordination chemistry.¹⁸ Thus, unlike their organometallic siblings, they are almost always better considered as clusters. For this reason it is not surprising that the development of metallaborane chemistry only blossomed with the discovery of the cluster electron counting rules.^{19–25} This valuable paradigm first provided a connection between molecular stoichiometry and geometric structure for both polyhedral boranes and metal clusters – connections that were not apparent with two- and three-center bond ideas alone.²⁶ With these rules reasonable structures could be derived from a molecular formula: structures which could then be spectroscopically tested. Secondly, the paradigm opened a way to a similar understanding of mixed main group–transition metal clusters. That is, with the addition of the idea of isolobal main group and transition metal fragments so useful in organometallic chemistry,^{27,28} the rules accommodated a wide variety mixed main group–transition metal

compositions and structures that are superbly exemplified by the metallaboranes.

Although the electron counting rules suggest a wide variety of target metallaborane compositions, they provided no direct information on synthesis. The key to overcoming the intrinsic instability of the M–B bond network relative to a mixture of separate boranes and metal complexes is to lower all free energy barriers in the preparative pathway below those of decomposition pathways. Our successful approach utilizes the ready formation of metal polyborohydrides either from metathesis of metal halogen bonds with metal borohydrides or by M–X, B–H bond metathesis with neutral boranes.²⁹ H_2 elimination from the polyborohydride in preference to borane elimination leads to metallaboranes. This approach has been successful for metallaboranes containing a variety of group 6–9 metals with the pentamethylcyclopentadienyl ancillary ligand on the metal. Thus, for the first time this route provided access to the chemistry of earlier transition metal compounds and yielded a variety of structural types, many having novel cage geometries or other structural features of unusual interest.³⁰

As yields are good, these metallaboranes constitute subjects for further reaction chemistry and that with Lewis bases and alkynes has been found most profitable.^{31,32} Most recently, easily displaced metal fragments have provided an example of metal assisted alkyne addition to a cluster framework.³³ However, we have also succumbed to the temptation to go back to our research roots and look at thermally driven borane cluster building on the different metallaborane frameworks. Yields are poor and selectivities low but these drawbacks are acceptable simply because the approach generates new cluster types, *e.g.*, syntheses of dirhenaboranes $(\eta^5\text{-C}_5\text{Me}_5\text{Re})_2\text{B}_n\text{H}_n$, $n = 7\text{--}10$ and diruthenaboranes, $(\eta^5\text{-C}_5\text{Me}_5\text{Ru})_2\text{B}_n\text{H}_{12}$ ($n = 6$ and 8).^{34–36} Here we report the results of the

^aDepartment of Chemistry, Indian Institute of Technology, Madras, Chennai, 600036, India

^bDepartment of Chemistry and Biochemistry, University of Notre Dame, Notre Dame, IN, 46556, USA

† Dedicated to Professor Ken Wade on the occasion of his 75th birthday.

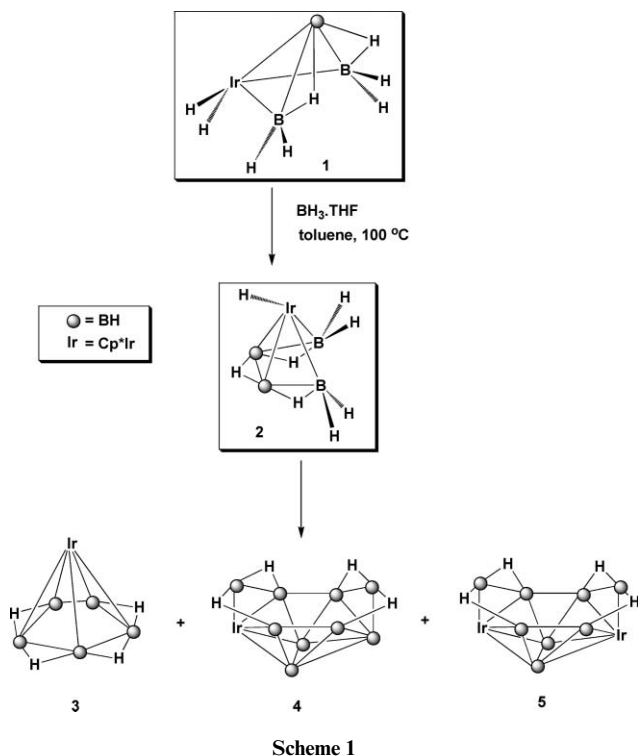
‡ CCDC reference numbers 662576–662579. For crystallographic data in CIF or other electronic format see DOI: 10.1039/b715040g

condensation of monoboranes with an iridatetraborane. Although group 9 cobaltaboranes constitute some of the earliest ones studied in a systematic way,^{4,37–39} there are important differences with rhoda- and iridaboranes.^{40–42} Specifically, the iridaboranes have a greater tendency to appear as monometallic clusters which are hydrogen-rich relative to their lighter metal congeners. Thus, *arachno*- $\{\eta^5\text{-C}_5\text{Me}_5\text{IrH}_2\}\text{B}_3\text{H}_7$, **1**, is an important product of our synthetic approach and reaction of **1** with $\text{BH}_3\cdot\text{THF}$ under mild conditions yields *arachno*- $\{\eta^5\text{-C}_5\text{Me}_5\text{IrH}\}\text{B}_4\text{H}_9$, **2**.^{32,42} Some questions explored here are whether larger iridaboranes are accessible at higher temperatures and whether there are any mechanistic similarities in the cluster expansion reactions for metallaboranes as a function of metal identity.

Results and discussion

Stable products

Thermolysis of $\{\eta^5\text{-C}_5\text{Me}_5\text{Ir}\}\text{B}_3\text{H}_9$, **1**, with $\text{BH}_3\cdot\text{THF}$ at 100 °C for 18 h followed by chromatography allows the isolation of three new stable metallaboranes ($\eta^5\text{-nido-C}_5\text{Me}_5\text{Ir}\}\text{B}_5\text{H}_9$, **3**, *nido*- $(\eta^5\text{-C}_5\text{Me}_5\text{Ir})\text{B}_9\text{H}_{13}$, **4**, and *nido*- $(\eta^5\text{-C}_5\text{Me}_5\text{Ir})_2\text{B}_8\text{H}_{12}$, **5** each in a yield of approximately 10% (Scheme 1). The known sole product at lower temperature ($\eta^5\text{-C}_5\text{Me}_5\text{Ir}\}\text{B}_4\text{H}_{10}$, **2**, is also formed. Descriptions of the characterizations of **3–5** from mass spectrometric, NMR, and X-ray diffraction studies follow.



nido-1- $(\eta^5\text{-C}_5\text{Me}_5\text{Ir})\text{B}_5\text{H}_9$, **3**

The mass spectrometric data for **3** show a molecular ion peak at 391 corresponding to a composition $(\eta^5\text{-C}_5\text{Me}_5\text{Ir})\text{B}_5\text{H}_9$. This formula and the cluster electron counting rules suggest a *nido*-cluster structure analogous to that of B_6H_{10} , *i.e.*, eight skeletal

electron pairs (sep) and a cluster structure based on a pentagonal bipyramid with one vertex unoccupied. Two isomers are likely depending on whether the metal fragment is located in the 1-position (apical) or 2-position (basal). The ^{11}B spin decoupled ^1H NMR spectrum at 22 °C shows, in addition to the resonance at 1.74 ppm due to cyclopentadienyl methyl protons, only one resonance at 3.3 ppm for five terminal hydrogens (left hand side of Fig. 1) and only one resonance at -4.9 ppm for the four bridging hydrogens (right hand side of Fig. 1). Similarly, the ^{11}B NMR spectrum at 22 °C (Fig. 2) consists of a single doublet at -1.8 ppm which collapses to a sharp singlet upon proton decoupling. Thus, neither isomer fits unless the cluster displays fluxional behavior at room temperature. A similar behavior at ambient temperature has previously been observed for hexaborane(10) and has been found to arise from a rapid intramolecular migration of the bridging hydrogens about the basal boron ring.⁴³ The room-temperature data on **3** do tend to rule out the 2-isomer as boron fluxionality in a *nido*-structure is unlikely. Hence, a 1-isomer that displays hydrogen fluxionality is most likely.

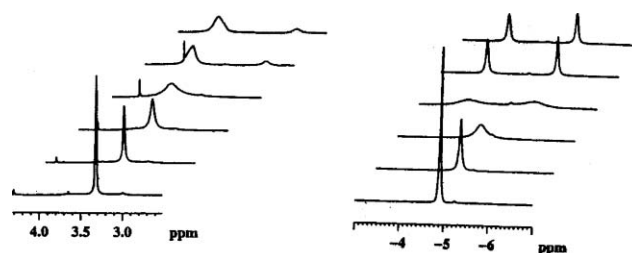


Fig. 1 Variable-temperature $\{^{11}\text{B}\}^1\text{H}$ NMR spectra of **3** in d_8 -toluene with the -100 °C spectrum at the top and the 22 °C spectrum at the bottom.

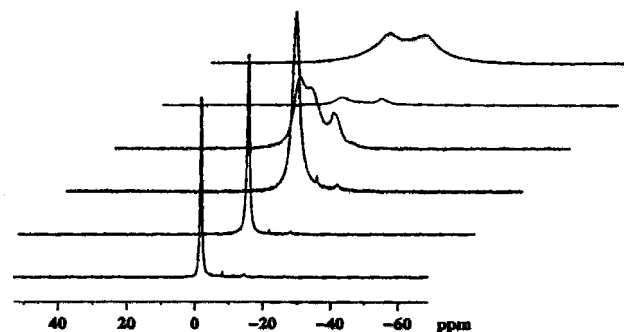


Fig. 2 Variable-temperature $\{^1\text{H}\}^{11}\text{B}$ NMR spectra of **3** in d_8 -toluene with the -100 °C spectrum at the top and the 22 °C spectrum at the bottom.

A static 1-isomeric form of **3** with five B–H terminal hydrogens and four B–H–B bridging hydrogens should possess three types of terminal basal B–H groups and two types of bridging hydrogens whereas the static 2-isomer would exhibit five types of B–H, three types of B–H–B and one B–H–Ir (or terminal Ir–H). The $\{^{11}\text{B}\}^1\text{H}$ NMR spectra were obtained over the range of 22 to -100 °C. As may be seen from Fig. 1, the B–H–B hydrogen resonance broadens and forms two distinct peaks at -4.0 and -5.6 ppm at the lowest temperature. Likewise the terminal resonances split into two peaks at 3.90 and 2.83 ppm, with the upfield peak exhibiting a poorly defined shoulder near 3.8 ppm. In the variable-temperature

{ ^1H } ^{11}B NMR spectra the single resonance observed at 22 °C broadens upon cooling forming three resonances (Fig. 2) at 1.1, 0.2 and -9.1 ppm of relative areas 2 : 2 : 1 at -60 °C. At even lower temperatures these resonances broaden further as the solvent become more viscous near its freezing point. These data are consistent with a *nido*-1-(η^5 - $\text{C}_5\text{Me}_5\text{Ir}$) B_5H_9 structure for the product.

The solid-state structure of **3**, shown in Fig. 3, confirms that the structure is the same as that in solution. Bond distances and angles are within normal ranges for metallaboranes of this type. In conformance with the cluster counting rules, this 8 sep cluster exhibits a structure based on a pentagonal bipyramid with an apical vertex unoccupied. Note that the electron counting rules permit an isomeric cluster geometry formed by leaving an equatorial vertex of the pentagonal bipyramid unoccupied. Although not known for boranes, a pair of isomers of this type has been described for dimetallacarboranes.⁴⁴

Five previous examples of metallaboranes analogous to **3** have been reported; 2-(CO) $_3\text{MnB}_5\text{H}_{10}$,⁵ 1-(η^5 - $\text{C}_5\text{Me}_5\text{Fe}$) B_5H_{10} ,⁴⁵ 2-(η^5 - $\text{C}_5\text{Me}_5\text{Fe}$) B_5H_{10} ,⁴⁵ 2-(CO) $_3\text{FeB}_5\text{H}_9$,⁴⁶ and 1-(η^5 - $\text{C}_5\text{Me}_5\text{Co}$) B_5H_9 .⁴⁷ To the best of our knowledge, our solid-state structure determination of **3** is the first for a *nido*-1-MB $_5$ cluster composition and is important for the reasons given above. *Pileo*-{1,2-(η^5 - $\text{C}_5\text{Me}_5\text{Ir}$) $_2\text{B}_5\text{H}_5$ }⁴⁸ has also been reported by insertion of metal fragments into known polyborane cages, $\text{B}_5\text{H}_9^{2-}$, which consists of an octahedral Ir_2B_4 cluster with an additional BH group capping a BIr_2 triangle. The NMR data for **3** and the other 1-isomers are compared in Tables 1 and 2. The fluxional behavior of compound **3** is unusual and the fact that **3** may be considered an analogue of (η^5 - C_5H_5) $_2\text{Fe}$ (ferrocene) because the $\text{B}_5\text{H}_9^{2-}$ “ligand” is isoelectronic

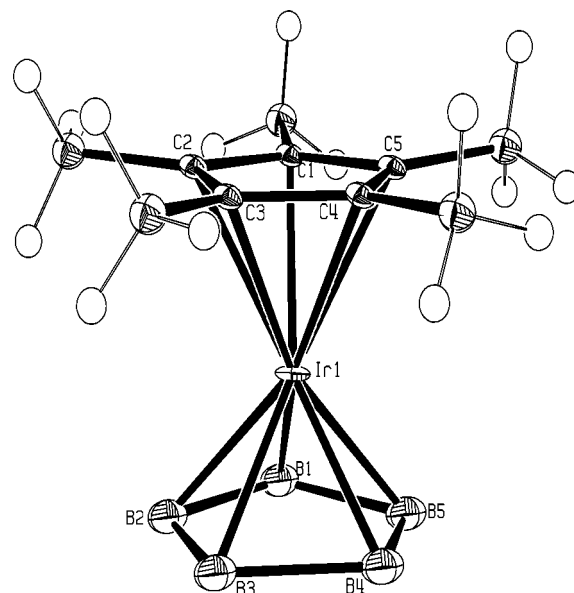


Fig. 3 Molecular structure of (η^5 - $\text{C}_5\text{Me}_5\text{Ir}$) B_5H_9 , **3**. Selected bond lengths (Å) and angles (°): Ir(1)–B(1) 2.17(3), Ir(1)–B(2), 2.20(3), Ir(1)–B(3) 2.16(3), Ir(1)–B(4) 2.16(3), Ir(1)–B(5) 2.17(3), Ir(1)–C(1) 2.23(2), Ir(1)–C(2) 2.26(2), C(1)–C(2) 1.43(3), B(3)–B(4) 1.88(4), B(1)–B(2) 1.74(4), B(1)–B(5) 1.80(4), B(4)–B(5) 1.83(4), B(2)–B(3) 1.78(5); B(4)–Ir(1)–B(3) 51.6(11), B(4)–Ir(1)–B(1) 86.3(11), B(3)–Ir(1)–B(5) 84.1(10), B(2)–B(1)–B(5) 109(2), B(5)–B(1)–Ir(1) 65.7(14), B(3)–Ir(1)–C(3) 102.4(8).

with the η^5 - C_5H_5^- ligand illustrates a connection to organometallic chemistry.

nido-3-(η^5 - $\text{C}_5\text{Me}_5\text{Ir}$) B_9H_{13} , **4**

The spectroscopic data for compound **4** plus straightforward application of the electron counting rules generate a structure for the metallaborane in solution and it was confirmed by an X-ray structure in the solid state. Thus, the mass spectrometric data show a molecular ion peak at 433 leading to a composition (η^5 - $\text{C}_5\text{Me}_5\text{Ir}$) B_9H_{13} with a total of 12 sep. According to the counting rules the structure should be *nido*-(η^5 - $\text{C}_5\text{Me}_5\text{Ir}$) B_9H_{13} based on an 11-vertex deltahedron with the vertex of connectivity 6 unoccupied. The “extra” bridging hydrogens are expected to be

Table 1 ^{11}B NMR Data for *nido*-MB $_5$ metallaboranes^{a,b}

Compound	δ_{B}^b (25 °C)/ppm (J/Hz)	δ_{B} (-100 °C)/ppm
1-(η^5 - C_5Me_5) $\text{FeB}_5\text{H}_{10}$	5.1 (145)	—
1-(η^5 - C_5Me_5) $\text{RuB}_5\text{H}_{10}$	-0.6 (151)	—
1-(η^5 - C_5Me_5) $\text{CoB}_5\text{H}_{10}$ ^c	12.8	15.2, 4.8 ^d
1-(η^5 - C_5Me_5) $\text{IrB}_5\text{H}_{10}$	-1.8 (148)	1.1, 0.2, -9.1

^a Unless noted otherwise spectra obtained in toluene- d_8 solution. ^b Parts per million relative to $\text{BF}_3\cdot\text{O}(\text{C}_2\text{H}_5)_2$. ^c Spectra obtained in CD_2Cl_2 solution. ^d Spectra obtained in CD_2Cl_2 solution at -70 °C.

Table 2 ^1H NMR Data for *nido*-MB $_5$ metallaboranes^a

Compound	δ_{H} (25 °C)/ppm	Assignment	δ_{H} (-100 °C)/ppm
1-(η^5 - C_5H_5) $\text{FeB}_5\text{H}_{10}$	4.23 s	C_5H_5	—
	3.50 s	$\text{B}-\text{H}_i$	—
	-4.52 br s	$\text{B}-\text{H}-\text{B}$	—
1-(η^5 - C_5Me_5) $\text{RuB}_5\text{H}_{10}$	1.83 s	C_5Me_5	—
	3.76 s	$\text{B}-\text{H}_i$	—
	-5.78 br s	$\text{B}-\text{H}-\text{B}$	—
1-(η^5 - C_5H_5) $\text{CoB}_5\text{H}_{10}$ ^b	4.89 s	C_5H_5	4.89 ^c
	3.78 s	$\text{B}-\text{H}_i$	3.93, 3.34, 3.11
	-4.59 br s	$\text{B}-\text{H}-\text{B}$	-3.39, -5.87
1-(η^5 - C_5Me_5) $\text{IrB}_5\text{H}_{10}$	1.74 s	C_5Me_5	1.74
	3.32 s	$\text{B}-\text{H}_i$	3.90, 3.75, 2.83
	-4.91 br s	$\text{B}-\text{H}-\text{B}$	-4.04, -5.57

^a Unless noted otherwise spectra obtained in toluene- d_8 solution. ^b Spectra obtained in CD_2Cl_2 solution. ^c Spectra obtained in CD_2Cl_2 solution at -70 °C.

located on the six-membered ring of the open face. Out of the four metal positional isomers possible, the NMR data eliminates two. The ^{11}B NMR spectrum shows six types of BH environments in a 1 : 2 : 1 : 2 : 2 : 1 ratio requiring a plane of symmetry for a static structure. Furthermore, the ^1H NMR spectrum shows, in addition to the Cp* ligand and terminal B–H resonances, two distinct B–H–B groups in a ratio of 2 : 2. Hence, the postulated structure is either *nido*-1- or *nido*-3-($\eta^5\text{-C}_5\text{Me}_5\text{Ir}$) B_9H_{13} .

In the solid state, the correct molecular structure of **4**, shown in Scheme 1 and Fig. 4, is demonstrated to be *nido*-3-($\eta^5\text{-C}_5\text{Me}_5\text{Ir}$) B_9H_{13} . Again, bond distances and angles are within normal ranges for metallaboranes of this type and the framework is that of $\text{B}_{10}\text{H}_{14}$ with a BH group in the 3-position replaced by an isolobal ($\eta^5\text{-C}_5\text{Me}_5$)Ir fragment. It is analogous to the previously described cobaltaborane ($\eta^5\text{-C}_5\text{H}_5\text{Co}$) B_9H_{13} .⁴⁷ The molecular structure of *nido*-3-($\eta^5\text{-C}_5\text{Me}_5\text{Ir}$) B_9H_{13} , **4** is also isostructural with the 1- and 2-isomers of *nido*-[($\eta^6\text{-C}_6\text{Me}_6$) $\text{RuB}_9\text{H}_{13}$].⁴⁹

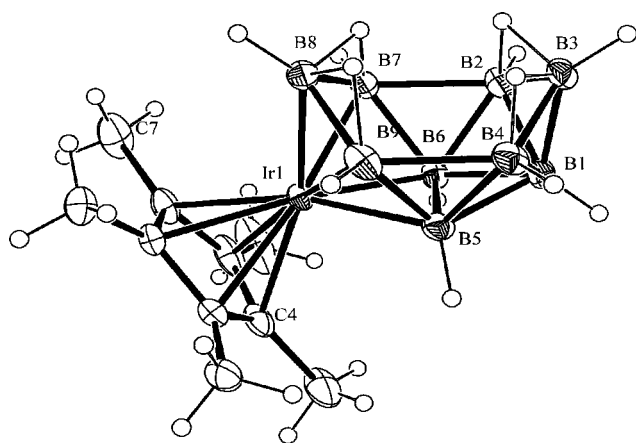


Fig. 4 Molecular structure of ($\eta^5\text{-C}_5\text{Me}_5\text{Ir}$) B_9H_{13} , **4**. Selected bond lengths (Å) and angles ($^\circ$): Ir(1)–B(8) 2.078(2), Ir(1)–B(6) 2.156(2), B(1)–B(3) 1.710(3), B(1)–B(5) 1.800(3), B(2)–B(7) 1.974(3), B(4)–B(9) 1.983(4), B(7)–B(8) 1.858(3), B(8)–B(9) 1.861(4); B(8)–Ir(1)–B(9) 52.17(11), B(8)–Ir(1)–B(5) 90.10(9), B(3)–B(1)–B(2) 61.44(14), B(2)–B(1)–B(4) 105.04(16), B(5)–B(1)–B(6) 61.11(13), B(6)–B(2)–B(3) 110.60(17), B(1)–B(3)–B(2) 61.09(14).

nido-3,4-($\eta^5\text{-C}_5\text{Me}_5\text{Ir}$) $_2\text{B}_8\text{H}_{12}$, **5**

In the same manner as compound **4**, a third product, **5**, was isolated and characterized spectroscopically and with an X-ray structure determination. The mass spectrometric data suggest a molecular formula of ($\eta^5\text{-C}_5\text{Me}_5\text{Ir}$) $_2\text{B}_8\text{H}_{12}$ with 12 sep. Again a *nido*-structure based on an 11-vertex deltahedron with the vertex of connectivity 6 unoccupied is generated by the electron counting rules. The ^{11}B NMR data (three resonances in the ratio 2 : 2 : 4) suggests a structure, if static, of higher symmetry than compound **4**. Consistent with this observation, **5** shows only one kind of Cp* signal and one kind of B–H–B proton indicating the two metal fragments and all four bridging hydrogens on the open six-membered face are equivalent. Hence, the structure is assigned as *nido*-3,4-($\eta^5\text{-C}_5\text{Me}_5\text{Ir}$) $_2\text{B}_8\text{H}_{12}$ as shown in Scheme 1. The proposed solution structure of **5** is consistent with the solid state structure which is shown in Fig. 5. Again the bond distances and angles are within typical ranges. Like **4** the cluster geometry is that of $\text{B}_{10}\text{H}_{14}$ with the 3-, 4-BH fragments replaced with iridium fragments.

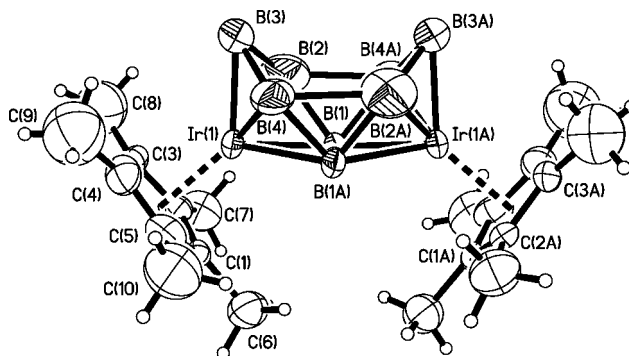


Fig. 5 Molecular structure of ($\eta^5\text{-C}_5\text{Me}_5\text{Ir}$) $_2\text{B}_8\text{H}_{12}$, **5**. Thermal ellipsoids at 50% probability. Selected bond lengths (Å) and angles ($^\circ$): Ir(1)–B(1A) 2.191(7), Ir(1)–B(1) 2.201(6), Ir(1)–B(4) 2.097(10), Ir(1)–B(3) 2.104(11), Ir(1)–B(2) 2.092(12), B(4)–B(1A) 1.825(13), B(3)–B(4) 1.927(18), B(1)–B(2) 1.793(15), B(2)–B(4A) 2.13(2); B(4)–Ir(1)–B(2) 90.8(6), B(4)–Ir(1)–B(3) 54.6(5), B(2)–Ir(1)–B(1) 49.3(5), B(4)–Ir(1)–B(1A) 50.3(4), B(2)–Ir(1)–B(1A) 86.4(5), B(2)–B(1)–Ir(1) 62.2(5). Symmetry equivalent positions denoted by “A” and generated by $-x, 1 - y, -z$.

The apparent metallaborane cluster condensation that produces **5** was observed previously in a tungstaborane system⁵⁰ and more recently an unambiguous example was demonstrated by showing that the reaction of ($\eta^5\text{-C}_5\text{Me}_5\text{Ir}$) B_3H_9 with ($\eta^5\text{-C}_5\text{Me}_5\text{Ru}$) $_2\text{B}_3\text{H}_9$ produces a diruthenairidaborane cluster.⁵¹ Hence, not only does borane addition result in increased cluster boron element nuclearity but cluster condensation must be considered an additional viable pathway for increasing both metal and boron element nuclearity in the cluster framework.

Intermediate products

A fourth fraction isolated from the product mixture (about 10% based on metal) decomposes in solution even at 0 $^\circ\text{C}$ which suggests the compound may play the role of an intermediate in the overall reaction process. Hence, despite its instability, characterization was attempted as these less stable species provide important hints to mechanism thereby justifying the greater expenditure of effort than for a stable material.

The mass spectrum of this product showed a molecular ion peak at 738 with an isotopic pattern consistent with a species containing minimally two Ir and seven boron atoms. The ^{11}B NMR spectrum shows seven types of boron environments in a ratio of 2 : 1 : 1 : 1 : 1 : 1 : 2 implying a total of nine boron atoms. In addition to two C_5Me_5 proton resonances of equal intensity, the $^1\text{H}\{^{11}\text{B}\}$ NMR spectrum reveals eight types of B–H protons (intensity total intensity 9.5 relative to a single C_5Me_5 resonance), the presence of one high-field Ir–H (intensity 0.9 relative to a single C_5Me_5 resonance), and four types of B–H–B protons (intensity total intensity 3.95 relative to a single C_5Me_5 resonance). These observations imply a total of 15 skeletal hydrogen atoms and an even electron composition of ($\eta^5\text{-C}_5\text{Me}_5\text{Ir}$) $_2\text{B}_9\text{H}_{15}$, **6**. With 14 sep, if counted as a single cage, the electron counting rules would require the structure to be based on a 13-vertex deltahedron with one vertex unoccupied. This is sufficiently unusual that the electron counting rules are less helpful than usual. In addition, the ready loss of borane from the parent ion, not seen in the other products, suggests a more complex structure. Hence the isolation of a crystal

suitable for a solid-state structure determination was important and the result is shown in Fig. 6.

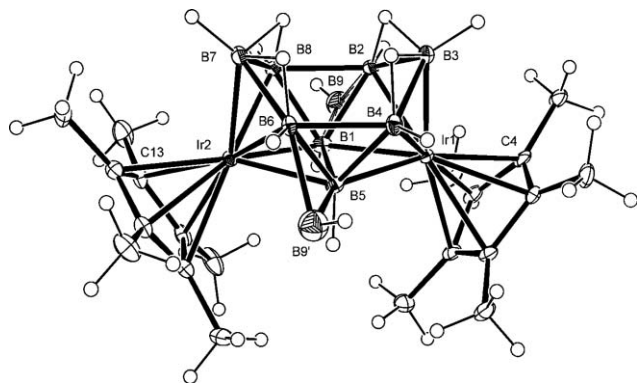


Fig. 6 Molecular structure of $(\eta^5\text{-C}_5\text{Me}_5\text{Ir})_2\text{B}_9\text{H}_{15}$, **6**. Selected bond lengths (Å) and angles ($^\circ$): Ir(1)–B(3) 2.078(7), Ir(1)–B(1) 2.178(7), Ir(2)–B(7) 2.068(7), B(1)–B(8) 1.791(10), B(1)–B(2) 1.805(10), B(1)–B(5) 1.913(9), B(1)–B(9) 2.00(4), B(2)–B(3) 1.870(10), B(2)–B(9) 1.97(4), B(2)–B(8) 1.985(11), B(5)–B(9) 1.76(5), B(6)–B(7) 1.862(10), B(6)–B(9) 1.89(4), B(3)–Ir(1)–B(2) 52.4(3), B(2)–Ir(1)–B(4) 85.8(3), B(5)–B(9)–B(6) 59.0(14), Ir(2)–B(5)–Ir(1) 127.1(3), B(9)–B(6)–Ir(2) 92.5(14).

As may be seen from Fig. 6 the cluster core has the same geometry as compound **5**, *i.e.*, a 12 sep *nido*-dimetalladecaborane. In addition, there are apparently two bridging monoborane groups positioned similarly to the single bridging borane observed previously in isostructural $(\eta^5\text{-C}_5\text{Me}_5\text{M})_2\text{B}_9\text{H}_{14}(\mu\text{-BH}_2)$, M = Ru, Re.³⁵ However, there is a problem with the solution. The composition refines to $(\eta^5\text{-C}_5\text{Me}_5\text{Ir})_2\text{B}_{8.5}\text{H}_{13}$ as the contribution of B(9) and B(9') is estimated to be 25% each! Note that the thermal ellipsoids are large so the actual contribution is probably somewhat smaller. There is a reasonable explanation for this puzzling observation. The two *exo*-polyhedral boron atoms of **6** bridge pairs of boron atoms in the main framework geometry that are related by a C_2 axis of symmetry. If there is only a single bridging borane as found with $(\eta^5\text{-C}_5\text{Me}_5\text{M})_2\text{B}_9\text{H}_{14}(\mu\text{-BH}_2)$, the structure could be disordered with equal population of the single B(9) on the symmetry equivalent sites (9) and (9'). This would put 50% of a boron atom on one bridging site. This accounts for half the discrepancy. It is also necessary to suggest that **6** co-crystallizes with compound **5** which has an identical heavy atom cluster structure and large $\eta^5\text{-C}_5\text{Me}_5$ ligands that could “hide” the bridging borane of **6** from neighboring molecules in the crystal. Incorporation of **5** may be due to a preferentially crystallized small impurity or formed by slow decomposition of **6** by loss of the bridging borane. Again recall the mass spectrometric results showing ready borane loss.

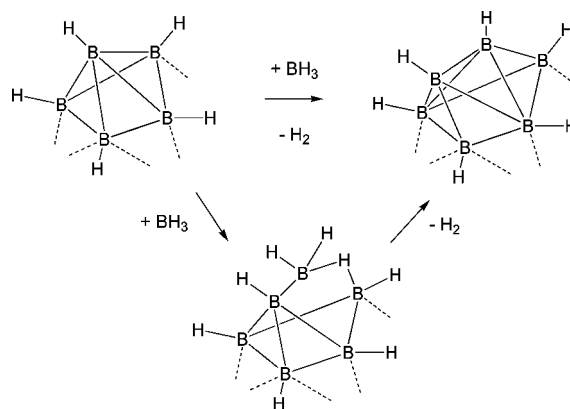
With these assumptions the structure solution is consistent with a molecular composition $(\eta^5\text{-C}_5\text{Me}_5\text{Ir})_2\text{B}_9\text{H}_{14}$ which would have one less H atom than that deduced from the NMR measurements as well as being an odd-electron structure. A look at the bridging borane in Fig. 6 shows that the bridging borane observed appears tetrahedral rather than the trigonal geometry expected for a true borylene.⁵² It is likely that there is in fact another hydrogen atom in the tetrahedral position for which was not found crystallographically. Thus, the bridging borane is judged to be

a BH_2 group as found earlier in the Ru and Re metallaboranes already mentioned.

Although the bridging monoborane found in **6** is very similar to that of $(\eta^5\text{-C}_5\text{Me}_5\text{M})_2\text{B}_9\text{H}_{14}(\mu\text{-BH}_2)$, M = Ru, Re, there is a difference. The framework of **6** contains a M–H hydrogen not present in the Ru or Re examples. Second, neither of the terminal hydrogens of the framework boron atoms adjacent to the bridging atom are engaged in B–H–B bonds with the bridging atom. We suggest **6** is formed simply by the addition of borane to **5**. Shift of the B–H–B hydrogen of the initial adduct to an Ir–B edge yields the structure observed for $(\eta^5\text{-C}_5\text{Me}_5\text{Ir})_2\text{B}_9\text{H}_{15}$. We already mentioned that the iridaborane network tends to retain hydrogen and formation of the Ir–H–B bridge stabilizes **6**. It would consequently make insertion a higher barrier process. Effectively this traps the species which then can be isolated. Compound **6**, then, is an excellent model for the active intermediate in a cluster expansion reaction albeit the hydrogen positions may be different. Its stability is consistent with the fact that no iridaboranes with greater than 10 cluster atoms were observed – the stepwise growth is terminated.

Cluster expansion pathway

Conventional wisdom suggests a principal stoichiometric pathway of cluster expansion of boranes as well as polyborane fragment growth in metallaborane clusters is a stepwise process of borane addition and H_2 loss as shown by the overall reaction in Scheme 2 for a borane framework. Structural definition of part of the mechanistic pathway resulted from the study of borane addition to $(\eta^5\text{-C}_5\text{Me}_5\text{Ru})_2\text{B}_9\text{H}_9$.³⁵ We were able to isolate two ruthenaborane expansion products with the same molecular formulae, *i.e.*, $(\eta^5\text{-C}_5\text{Me}_5\text{Ru})_2\text{B}_{10}\text{H}_{16}$. These are structural isomers one of which converts on heating to the other. However, the structural change is unusual and mechanistically significant. The less stable isomer contains an exopolyhedral BH_2 group connected to the main 11-framework atom cluster *via* B–B and B–H–B interactions. The ruthenaborane transformation illustrates simple insertion with no loss of H_2 . As illustrated in Scheme 2, such loss is required for retention of the cluster class, *e.g.*, *nido*- to *nido*-, where a single BH is added to the framework. The present results now confirm the first step of the mechanism: addition of borane to the cluster framework. No Ru_2B_7 metallaborane was observed in the earlier work and, thus, formation of $(\eta^5\text{-C}_5\text{Me}_5\text{Ru})_2\text{B}_{10}\text{H}_{16}$ was not proven



Scheme 2

to occur by borane addition. However, **6** certainly comes from the addition of borane to **5**. Thus, the present work completes an unambiguous determination of the two steps of cage expansion by borane given in Scheme 2. In essence, the cluster building pathway energetics are changed by changing the nature of the transition metal thereby “freezing out” selected intermediates along the pathway.

This mechanism derives additional richness from an unexpected source: the addition of an alkyne to $(\eta^5\text{-C}_5\text{Me}_5\text{Ru})_2\text{B}_3\text{H}_9$.⁴⁴ The product of interest here is $(\eta^5\text{-C}_5\text{Me}_5\text{Ru})_2\text{C}_2\text{R}_2\text{B}_2\text{H}_5(\mu\text{-BH}_2)$ which has been fully characterized structurally. The monoborane is connected *via* Ru-B and B-H-B bonds but otherwise similar to that found in $(\eta^5\text{-C}_5\text{Me}_5\text{Ru})_2\text{B}_{10}\text{H}_{16}$. On heating the compound undergoes loss of a monoborane fragment. The energetically uphill reverse process, *i.e.*, borane addition and alkyne elimination, can be viewed a model of a pathway for monoborane fragment growth on a ruthenacarbaborane. Thus, replacing alkyne with H₂ we have borane addition and H₂ elimination, *i.e.*, the path in Scheme 2. The difference in the energetics of the alkyne *vs.* H₂ systems would change the direction of the favorable pathway. Observation of an exopolyhedral BH₂ group in a variety of cluster compositions and structures add weight to the argument that it is indeed the key intermediate species in the cluster building reaction.

We conclude that cluster expansion takes place by monoborane addition external to the cluster framework. For any metal, the barrier for insertion apparently increases with increasing nuclearity and eventually becomes large relative to other possible reactions, *e.g.*, H shift to a metal site as found in **6**, so that cluster growth stops. A less frequently observed parallel path for growth is condensation of two metallaboranes, presumably *via* intermediate species that have not become stabilized by elimination or rearrangement. Clearly, the electron counting rules that spurred the development of this area of cluster chemistry by creating a transparent view of structure has led to significant understanding of cluster reactivity as well. It is the development of reactivity which will eventually lead to applications as well as new areas of exploration.

Experimental

General procedures

All the operations were conducted under an Ar/N₂ atmosphere using standard Schlenk techniques. Solvents were distilled prior to use under N₂. BH₃·THF, LiBH₄ in THF (Aldrich) were used as received. $(\eta^5\text{-C}_5\text{Me}_5\text{Ir})_2\text{B}_3\text{H}_9$, **1** was prepared as described previously.⁴² Chromatography was carried out on 3 cm of silica gel in a 2.5 cm diameter column. Thin layer chromatography was carried on 250 mm diameter aluminum supported silica gel TLC plates. NMR spectra were recorded on a 400 MHz Bruker FT-NMR spectrometer. Residual solvent protons were used as reference (δ , ppm, benzene, 7.15), while a sealed tube containing [Me₄N(B₃H₈)] in acetone-*d*₆ (δ _B, ppm, -29.7) was used as an external reference for the ¹¹B NMR. Infrared spectra were obtained on a Nicolet 205 FT-IR spectrometer. Mass spectra were obtained on JEOL JMS-AX505HA mass spectrometer with perfluoro kerosene as standard. Crystal data were collected and integrated using a Bruker Apex system with graphite monochromated

Mo-K α ($\lambda = 0.71073 \text{ \AA}$) radiation at 100 K. The structures were solved by heavy atom methods and refined by least-squares.⁵³

Reaction of $(\eta^5\text{-C}_5\text{Me}_5\text{Ir})\text{B}_3\text{H}_9$, **1**, with BH₃·THF

1 (0.25 g, 0.67 mmol) in toluene (20 mL) was stirred with 6 equivalents of BH₃·THF (4.01 mL, 4.02 mmol) for 18 h at 100 °C. The solvent was removed *in vacuo*; the residue was extracted in hexane, and passed through Celite. The filtrate was removed and the residue was sublimed. The colorless sublimation product was collected and chromatographed on silicagel TLC plates. Elution with pure hexane yielded two well separated colorless compounds: $(\eta^5\text{-C}_5\text{Me}_5\text{Ir})\text{B}_4\text{H}_{10}$, **2** (0.11 g, 45%) and $(\eta^5\text{-C}_5\text{Me}_5\text{Ir})\text{B}_5\text{H}_9$, **3** (0.03 g, 12%). The residue left after sublimation was dissolved in hexane-CH₂Cl₂ (8 : 2 v/v) and passed through Celite. The filtrate was concentrated and chromatographed on silicagel TLC plates. Elution with hexane-CH₂Cl₂ (9 : 1) yielded three colorless compounds: $(\eta^5\text{-C}_5\text{Me}_5\text{Ir})\text{B}_9\text{H}_{13}$, **4** (0.02 g, 7%), $(\eta^5\text{-C}_5\text{Me}_5\text{Ir})_2\text{B}_8\text{H}_{12}$, **5** (0.08 g, 16%) and $(\eta^5\text{-C}_5\text{Me}_5\text{Ir})_2\text{B}_9\text{H}_{15}$, **6** (0.05 g, 10%).

Selected data for $(\eta^5\text{-C}_5\text{Me}_5\text{Ir})\text{B}_5\text{H}_9$, **3.** MS (FAB) P⁺(max) 391 (isotopic pattern for 1 Ir and 5 B atoms); mass: calc. for ¹²C₁₀¹H₂₄¹¹B₅¹⁹²Ir 391.1973; obs. 391.1994. ¹¹B NMR (C₆D₆, 22 °C): δ -1.79 (d, $J_{\text{B-H}} = 148 \text{ Hz}$, 5B); ¹H NMR (C₆D₆, 22 °C): δ 3.32 (partially collapsed quartet (pcq), 5 BH_i), 1.74 (s, 15H, Cp*), -4.91 (quartet on ¹H-¹¹B decoupling, 4B-H-B); IR (hexane, cm⁻¹): 2506w, 2419w (B-H_i). Elemental analysis (%) for C₁₀H₂₄B₅Ir, C: calc. 30.75, obs. 31.02; H: calc. 6.19, obs. 6.40.

Selected data for $(\eta^5\text{-C}_5\text{Me}_5\text{Ir})\text{B}_9\text{H}_{13}$, **4.** MS (FAB) P⁺(max) 433 (isotopic pattern for 1 Ir and 9 B atoms); mass: calc. for ¹²C₁₀¹H₂₈¹¹B₉¹⁹²Ir 438.2580; obs. 438.2607. ¹¹B NMR (C₆D₆, 22 °C): δ 12.9 (d, $J_{\text{B-H}} = 131 \text{ Hz}$, 1BH_i), 9.1 (d, $J_{\text{B-H}} = 139 \text{ Hz}$, 2BH_i), -2.58 (d, $J_{\text{B-H}} = 146 \text{ Hz}$, 1BH_i), -3.93 (d, $J_{\text{B-H}} = 152 \text{ Hz}$, 2BH_i), -10.99 (d, $J_{\text{B-H}} = 148 \text{ Hz}$, 2BH_i), -43.45 (d, $J_{\text{B-H}} = 149 \text{ Hz}$, 1BH_i); ¹H NMR (C₆D₆, 22 °C): δ 5.31 (pcq, 1 BH_i), 4.48 (pcq, 2BH_i), 3.64 (pcq, 3BH_i), 2.44 (pcq, 2BH_i), 1.65 (pcq, 1BH_i), 1.66 (s, 15 H, 1Cp*), -2.35 (s, br, 2B-H-B), -4.08 (pcq, 2B-H-B); IR (hexane, cm⁻¹): 2508w, 2428w (B-H_i).

Selected data for $(\eta^5\text{-C}_5\text{Me}_5\text{Ir})_2\text{B}_8\text{H}_{12}$, **5.** MS (FAB) P⁺(max) 753 (isotopic pattern for 2 Ir and 8 B atoms); mass: calc. for ¹²C₂₀¹H₄₂¹¹B₈¹⁹²Ir₂: 755.3250; obs. 755.3212. ¹¹B NMR (C₆D₆, 22 °C): δ 1.82 (d, $J_{\text{B-H}} = 136 \text{ Hz}$, 2 BH_i), -0.24 (d, $J_{\text{B-H}} = 144 \text{ Hz}$, 2 BH_i), -12.89 (d, $J_{\text{B-H}} = 130 \text{ Hz}$, 4BH_i); ¹H NMR (C₆D₆, 22 °C): δ 5.82 (pcq, 2 BH_i), 4.12 (pcq, 2BH_i), 2.77 (pcq, 4BH_i), 1.78 (s, 30 H, 2Cp*), -3.73 (br, 4B-H-B); IR (hexane, cm⁻¹): 2492w, 2430w (B-H_i).

Selected data for $(\eta^5\text{-C}_5\text{Me}_5\text{Ir})_2\text{B}_9\text{H}_{15}$, **6.** MS (FAB) P⁺(max) 738; ¹¹B NMR (C₆D₆, 22 °C): δ 0.4 (d, $J_{\text{B-H}} = 138 \text{ Hz}$, 2 BH), -2.6 (d, $J_{\text{B-H}} = 139 \text{ Hz}$, 1 BH), -4.1 (d, $J_{\text{B-H}} = 146 \text{ Hz}$, 1 BH), -6.1 (d, $J_{\text{B-H}} = 144 \text{ Hz}$, 1 BH), -8.2 (br, 1 BH), -9.3 (d, $J_{\text{B-H}} = 149 \text{ Hz}$, BH), -10.5 (d, $J_{\text{B-H}} = 151 \text{ Hz}$, 2 BH); ¹H NMR (C₆D₆, 22 °C): δ 5.52 (pcq, BH_i), 4.34 (pcq, BH_i), 3.64 (pcq, BH_i), 3.37 (pcq, BH_i), 3.22 (pcq, BH_i), 2.99 (pcq, BH_i), 2.33 (pcq, BH_i), 2.23 (pcq, BH_i), 1.72 (s, 15 H, Cp*), 1.71 (s, 15 H, Cp*), -2.89 (br, B-H-B), -3.94 (br, B-H-B), -4.01 (br, B-H-B), -4.62 (br, B-H-B), -15.92 (s, Ir-H); IR (hexane, cm⁻¹): 2490w, 2424w (B-H_i).

Table 3 Crystallographic data and structure refinement details for compounds 3–6

	3	4	5	6
Chemical formula	C ₁₀ H ₂₄ B ₃ Ir	C ₁₀ H ₂₈ B ₉ Ir	C ₂₀ H ₄₂ B ₈ Ir ₂	C ₂₀ H ₄₃ B _{8.50} Ir ₂
<i>M_r</i>	390.54	437.81	753.42	759.83
Space group	<i>P</i> 2 ₁ / <i>n</i>	<i>P</i> 2 ₁ / <i>n</i>	<i>Fdd</i> 2	<i>P</i> 2 ₁ / <i>n</i>
<i>a</i> /Å	7.1589(8)	8.3313(1)	40.5755(5)	8.3424(2)
<i>b</i> /Å	12.9831(18)	16.0536(2)	8.3206(1)	15.4752(3)
<i>c</i> /Å	15.790(2)	13.2029(2)	15.3233(2)	19.7068(4)
β /°	99.888(10)	100.745(1)	90	94.178(1)
<i>V</i> /Å ³	1445.8(3)	1734.89(4)	5173.34(11)	2537.39(9)
<i>Z</i>	4	4	8	4
<i>T</i> /°C	100(2)	200(2)	100(2)	100(2)
λ /Å	0.71073	0.71073	0.71073	0.71073
<i>D_c</i> /g cm ⁻³	1.794	1.676	1.935	1.989
μ /cm ⁻¹	9.203	7.676	10.285	10.485
Reflections coll'd/unique	12979/4739	26137/6500	56061/6195	96994/9056
Reflections obs'd	4597	5776	5403	7224
<i>R</i> _{int}	0.0481	0.0256	0.0344	0.0551
<i>R</i> 1 (<i>F</i> ² , <i>I</i> > 2σ(<i>I</i>))	0.0783	0.0187	0.0291	0.0364
<i>wR</i> 2 (<i>F</i> ²)	0.2131	0.0470	0.0656	0.0826
<i>S</i>	1.245	1.116	1.078	1.226

$wR2 = \{\sum[w(F_o^2 - F_c^2)^2]/\sum[w(F_o^2)^2]\}^{1/2}$; $R1 = \sum||F_o| - |F_c||/\sum|F_o|$; $S = \{\sum[w(F_o^2 - F_c^2)^2]/(n - p)\}^{1/2}$; *n* = number of reflections, *p* = number of parameters refined

X-Ray structure determination

Crystallographic information for compounds 3–6 is given in Table 3. Preliminary examination and data collection were performed on Bruker D8-Apex diffractometer equipped with an Oxford Cryosystems 700 Series low-temperature apparatus operating at 100 K. Cell parameters were determined using reflections harvested from three orthogonal sets of 20 0.5° ϕ scans and refined with reflections from the entire data collection. Indexing of the non-merohedral twins was performed with *Cell_Now*.⁵⁴ Data collection strategies were calculated using *COSMO*.⁵⁵ All the structures were solved by heavy atom methods and refined by the method of least squares.⁵⁵

(η^5 -C₅Me₅Ir)B₃H₉, **3**. This crystal is a three-component non-merohedral twin in space group *P*2₁/*n* (no. 14). The scale factors for the second and third components are 0.323(3) and 0.312(2), respectively. The structure was solved using data from the first twin component only. After refining to near completeness, the second and third components were added. It appears that there is substitution disorder between the boron ring and the Cp*; parameters for thermal motion were inconsistent for all B and C atoms. CCDC 662578.

(η^5 -C₅Me₅Ir)B₉H₁₃, **4**. The asymmetric unit, and molecular structure, is an Ir bound to a Cp* and a B₉H₁₃ cage. Hydrogens attached to boron were located by difference Fourier map and freely refined in subsequent cycles of least-squares refinement. Structure solution by direct methods in centrosymmetric space group *P*2₁/*c* (no. 14), revealed the non-hydrogen structure. CCDC 662579.

(η^5 -C₅Me₅Ir)₂B₈H₁₂, **5**. Cell parameters were refined using 7932 reflections with *I* ≥ 10σ(*I*) and 4.02 ≤ θ ≤ 35.07° harvested from the entire data collection. Data were measured to 0.60 Å. In total, 56061 reflections were measured, 6195 unique, 5403 observed, *I* > 2σ(*I*). All data were corrected for Lorentz and polarization effects as well as for absorption. The asymmetric unit

in space group *Fdd*2 (no. 43) is 1/2 molecule. The metal position and the boron positions were found in the initial solution; the carbon positions were found by difference map during subsequent cycles of least-squares refinement. CCDC 662577.

(η^5 -C₅Me₅Ir)₂B₉H₁₅, **6**. Cell parameters were refined using 9204 reflections with *I* ≥ 10σ(*I*) and 2.63 ≤ θ ≤ 36.32° harvested from the entire data collection. In total, 96994 reflections were measured, 9056 unique, 7224 observed, *I* > 2σ(*I*). After solution by Patterson function in space group *P*2₁/*n* (no. 14), borons and missing methyl carbons were located by subsequent cycles of least-squares refinement followed by difference Fourier synthesis. All non-hydrogen atoms were refined with parameters for anisotropic thermal motion. Borons B9 and B9' were persistent residual peaks in the difference map. They were modeled at 25% site occupancy and could not be modeled with anisotropic thermal parameters. CCDC 662576.

Acknowledgements

The support of the National Science Foundation under grant 0304008 is gratefully acknowledged.

References

- 1 N. N. Greenwood and I. M. Ward, *Chem. Soc. Rev.*, 1974, **3**, 231.
- 2 R. N. Grimes, *Acc. Chem. Res.*, 1978, **11**, 420.
- 3 R. N. Grimes, *Pure Appl. Chem.*, 1982, **54**, 43.
- 4 R. N. Grimes, in *Metal Interactions with Boron Clusters*, ed. R. N. Grimes, Plenum, New York, 1982, p. 269.
- 5 (a) J. D. Kennedy, *Prog. Inorg. Chem.*, 1984, **32**, 519; (b) J. D. Kennedy, *Prog. Inorg. Chem.*, 1986, **34**, 211.
- 6 J. D. Kennedy, in *Disobedient Skeletons*, ed. J. Casanova, New York, 1998.
- 7 D. F. Gaines, in *Recent Advances in the Chemistry of Pentaborane(9)*, ed. R. W. Parry and G. Kodama, Oxford, 1980.
- 8 (a) L. Barton, D. K. Srivastava, in *Comprehensive Organometallic Chemistry II*, ed. E. Abel, F. G. A. Stone and G. Wilkinson, Pergamon, New York, 1995, vol 1; (b) R. N. Grimes, in *Comprehensive*

- Organometallic Chemistry II*, ed. E. Abel, F. G. A. Stone and G. Wilkinson, Pergamon, New York 1995, vol 1, ch. 9.
- 9 S. J. Hildebrandt, D. F. Gaines and J. C. Calabrese, *Inorg. Chem.*, 1978, **17**, 790.
- 10 S. G. Shore, D.-Y. Jan, L.-Y. Hsu and W.-L. Hsu, *J. Am. Chem. Soc.*, 1983, **105**, 5923.
- 11 D.-Y. Jan, D. P. Workman, L.-Y. Hsu, J. A. Krause and S. G. Shore, *Inorg. Chem.*, 1992, **31**, 5123.
- 12 T. J. Coffy, G. Medford, J. Plotkin, G. J. Long, J. C. Huffman and S. G. Shore, *Organometallics*, 1989, **8**, 2404.
- 13 T. J. Coffy and S. G. Shore, *J. Organomet. Chem.*, 1990, **394**, C27.
- 14 J. J. Briguglio and L. G. Sneddon, *Organometallics*, 1985, **4**, 721.
- 15 D. E. Kadlecek, P. J. Carroll and L. G. Sneddon, *J. Am. Chem. Soc.*, 2000, **122**, 10686.
- 16 R. P. Micciche, P. J. Carroll and L. G. Sneddon, *Organometallics*, 1985, **4**, 1619.
- 17 R. N. Leyden, B. P. Sullivan, R. T. Baker and M. F. Hawthorne, *J. Am. Chem. Soc.*, 1978, **100**, 3758.
- 18 T. P. Fehlner, J.-F. Halet and J.-Y. Saillard, *Molecular Clusters. A Bridge to Solid-State Chemistry*, Cambridge University Press, Cambridge, 2007.
- 19 K. Wade, *Electron Deficient Compounds*, Nelson, London, 1971.
- 20 K. Wade, *Inorg. Nucl. Chem. Lett.*, 1972, **8**, 559.
- 21 K. Wade, *New Sci.*, 1974, **62**, 615.
- 22 K. Wade, *Adv. Inorg. Chem. Radiochem.*, 1976, **18**, 1.
- 23 D. M. P. Mingos, *Nature (London)*, 1972, **236**, 99.
- 24 D. M. P. Mingos and R. L. Johnston, *Struct. Bonding*, 1987, **68**, 29.
- 25 D. M. P. Mingos and D. J. Wales, *Introduction to Cluster Chemistry*, Prentice Hall, New York, 1990.
- 26 W. N. Lipscomb, *Boron Hydrides*, Benjamin, New York, 1963.
- 27 R. Hoffmann, *Science*, 1981, **211**, 995.
- 28 R. Hoffmann, *Angew. Chem., Int. Ed. Engl.*, 1982, **21**, 711.
- 29 T. P. Fehlner, *Proc. Indian Natl. Sci. Acad. A*, 2002, **68**, 579.
- 30 T. P. Fehlner, *Organometallics*, 2000, **19**, 2643.
- 31 X. Lei, M. Shang and T. P. Fehlner, *Organometallics*, 2000, **19**, 5266.
- 32 R. Macias, T. P. Fehlner and A. M. Beatty, *Angew. Chem., Int. Ed.*, 2002, **41**, 3860.
- 33 F. de Montigny, R. Macias, B. Noll, T. P. Fehlner, K. Costuas, J.-Y. Saillard and J.-F. Halet, *J. Am. Chem. Soc.*, 2007, **129**, 3392.
- 34 S. Ghosh, A. M. Beatty and T. P. Fehlner, *Angew. Chem., Int. Ed.*, 2003, **42**, 4678.
- 35 S. Ghosh, B. C. Noll and T. P. Fehlner, *Angew. Chem., Int. Ed.*, 2005, **44**, 2916.
- 36 L. Guennic, H. Jiao, S. Kahal, J.-Y. Saillard, J.-F. Halet, S. Ghosh, M. Shang, A. M. Beatty, A. L. Rheingold and T. P. Fehlner, *J. Am. Chem. Soc.*, 2004, **126**, 3203.
- 37 V. R. Miller, R. Weiss and R. N. Grimes, *J. Am. Chem. Soc.*, 1977, **99**, 5646.
- 38 R. Weiss and R. N. Grimes, *J. Am. Chem. Soc.*, 1977, **99**, 8087.
- 39 R. Weiss, J. R. Bowser and R. N. Grimes, *Inorg. Chem.*, 1978, **17**, 1522.
- 40 K. J. Deck, T. P. Fehlner and A. L. Rheingold, *Inorg. Chem.*, 1993, **32**, 2794.
- 41 X. Lei, M. Shang and T. P. Fehlner, *J. Am. Chem. Soc.*, 1999, **121**, 1275.
- 42 X. Lei, M. Shang and T. P. Fehlner, *Chem. Eur. J.*, 2000, **6**, 2653.
- 43 S. G. Shore, in *Polyhedral Boranes*, ed. E. L. Muetterties, Academic Press, New York, 1975.
- 44 H. Yan, A. M. Beatty and T. P. Fehlner, *J. Organomet. Chem.*, 2003, **680**, 66.
- 45 R. Weiss and R. N. Grimes, *Inorg. Chem.*, 1979, **18**, 3291.
- 46 T. P. Fehlner, J. D. Ragaini, M. Mangion and S. G. Shore, *J. Am. Chem. Soc.*, 1976, **98**, 7085.
- 47 R. Wileynski and L. G. Sneddon, *Inorg. Chem.*, 1979, **18**, 864.
- 48 J. Bould, N. P. Rath and L. Barton, *Organometallics*, 1995, **14**, 2119.
- 49 M. Bown, X. L. R. Fontaine, N. N. Greenwood, J. D. Kennedy and P. MacKinnon, *J. Chem. Soc., Chem. Commun.*, 1987, 817.
- 50 A. S. Weller, M. Shang and T. P. Fehlner, *J. Am. Chem. Soc.*, 1998, **120**, 8283.
- 51 I. J. Mavunkal, B. C. Noll, R. Meijboom, A. Muller and T. P. Fehlner, *Organometallics*, 2006, **25**, 2906.
- 52 H. Braunschweig, M. Forster, K. Radacki, F. Seeler and G. R. Whittell, *Angew. Chem., Int. Ed.*, 2007, **46**, 5212.
- 53 *Apex2*, Bruker AXS, Inc., Madison, WI, USA, 2004.
- 54 G. M. Sheldrick, *Cell Now*, University of Göttingen, Germany, 2004.
- 55 *COSMO*, Bruker AXS, Inc., Madison, WI, USA, 2004.